

## X-ray photoemission spectra of the valence bands of the 3d transition metals, Sc to Fe<sup>†</sup>

L. Ley,\* O. B. Dabbousi,† S. P. Kowalczyk,\* F. R. McFeely,§ and D. A. Shirley

*Materials and Molecular Research Division, Lawrence Berkeley Laboratory and Department of Chemistry, University of California, Berkeley, California 94720*

(Received 3 May 1977)

High-resolution x-ray-photoemission valence-band (VB) spectra are presented of the 3d transition metals, Sc to Fe. The measurements were conducted under ultra-high-vacuum conditions using polycrystalline samples. In the hcp elements Sc and Ti the main peaks in the valence bands are identified and compared with the results of band-structure calculations. Some rigidity is observed in the Sc and Ti bands as well as in the V and Cr bands. The expected two-peak structure for V and Cr is observed. In chromium we also observed a relatively low density of states at the Fermi energy. The VB spectrum for chromium is compared to theoretical predictions, and we present an assignment of the Cr symmetry-point energies. Our valence-band spectrum of Mn is quite similar to that of Hüfner and Wertheim and our spectrum of Fe is in good agreement with that observed by Höchst, Goldman, and Hüfner. These iron VB spectra agree qualitatively with expectations based on band models of ferromagnetism. It is observed that the VB spectrum of bcc iron may be constructed to agree within an energy scale factor from two bcc Cr VB's shifted to account for spin polarization. We also deduce the symmetry-point energies in iron.

### I. INTRODUCTION

The 3d transition elements comprise an interesting group of metals, exhibiting a wide variety of structural and electromagnetic properties. A key factor in the understanding of these metals is the peculiar nature of their electronic band structures. The valence bands may be considered to arise from the nearly degenerate 3d and 4s atomic levels. These levels have very different spatial distributions, with the 4s electrons extending considerably beyond the average radius of the 3d shell. Thus the valence bands of the 3d metals are of two distinct types, a wide band of predominately 4s character resembling the valence bands of simple metals, and a set of narrow, more correlated d-like bands. The s-like electrons are believed to be the primary source of bonding in the metals,<sup>1</sup> while the narrow atomiclike d bands give rise to such phenomena as ferromagnetism.<sup>2</sup>

Detailed and quantitative knowledge of the valence-band (VB) density of states (DOS),  $N(E)$ , is rather essential since many theories of the magnetic properties of the transition metals take d-band width, total band width and the DOS at the Fermi level as essential one-electron properties responsible for magnetic behavior. Electronic specific-heat data, conductivity measurements, and the de Haas-van Alphen effect, to mention only a few, sample the electronic properties only within  $\sim kT$  of the Fermi energy; thus information on the more tightly bound states is necessarily indirect. Spectroscopic methods such as soft-x-ray-emission spectroscopy (SXS),<sup>3-7</sup> ultraviolet and x-ray-photoemission (UPS, XPS),<sup>8-15</sup> and optical-reflectivity measurements are free of these limita-

tions and have contributed valuable information about the overall features of  $N(E)$  for most of the metals under consideration here.

A straightforward interpretation of SXS and low-energy ( $h\nu < 40$ -eV) UPS data in terms of only the initial density of states is rather difficult in most cases. In SXS, the initial-state core vacancy may distort the valence-band density of states severely. Examples of such distortions are well documented in the emission spectra of the alkali metals.<sup>16</sup> Low-energy uv photoemission spectra are commonly interpreted in one of two ways; the direct-transition model,<sup>17</sup> in which  $\vec{k}$  conservation is an important selection rule and the non-direct-transition model.<sup>18</sup> In either case the measured spectrum will contain features reflecting both the initial electron state and the final electron state subject to the restriction of energy conservation. Starting with a reliable band-structure calculation, an interpretation of the UPS spectrum in terms of initial- and final-state properties is possible, and it can yield very detailed results.<sup>19-21</sup>

XPS measurements, however, are free from such limitations, for with increasing excitation energy  $h\nu$ , the  $\vec{k}$  selection rule is readily fulfilled without introducing additional structure. This is expected from the high and uniform density of available states over the whole range of  $\vec{k}$  space at energies large compared to the energy variations of the lattice potential. Experimental evidence for this fact is well documented<sup>22</sup> and the interpretation of high-energy spectra in terms of initial-state density has been highly successful.<sup>23</sup>

In this report our objective is to present a systematic study of the density of states of the first-row transition metals Sc through Fe. In an un-

published earlier report,<sup>24</sup> results concerning these elements were presented. In that report, the positions of the Fermi levels for some of these metals were in error. The Fermi levels for these metals has been redetermined and some of the spectra have been repeated. This report, therefore, should supercede our previously reported data. Experimental details are given in Sec. II and results are presented in Sec. III. Of the elements reported here Fe (Refs. 15 and 25–28) and Mn (Ref. 27) have been studied earlier by XPS methods. We shall refer to these works and present a discussion of our results in Sec. IV.

## II. EXPERIMENTAL

All the specimens were studied in a Hewlett-Packard 5950A electron spectrometer with a monochromatized Al  $K\alpha$  (1486.6 eV) x-ray source. The instrumental resolution is 0.55(2) eV as previously measured from the broadening of the sharp Fermi edge of a number of metals.<sup>29</sup>

The spectrometer has been modified for ultrahigh-vacuum operation, and was baked out at 200 °C before the start of this series of experiments, obtaining a base pressure of  $\leq 2 \times 10^{-10}$  Torr. All the samples were prepared *in situ*. Films of Ti, V, Cr, Mn, and Fe were prepared by dc sputtering from high-purity single crystals onto stainless-steel substrates in an ultrapure argon atmosphere. Sc, Ti, and V specimens were prepared by vapor deposition onto stainless steel substrates. Ta or W filaments were used and the evaporation charges were either single crystals or ultrapure (better than 99.99%) polycrystalline material. Before evaporation, the filament and charge were vigorously outgassed. In most cases, the vacuum during evaporation was  $1 \times 10^{-9}$  Torr or better, and the worst case was  $5 \times 10^{-9}$  Torr. A bulk sample, cleaned with a mechanical scraper, was also used in the Cr case. The different methods of sample preparation gave identical valence band spectra. Each sample was checked for impurities such as imbedded argon, surface contaminants (oxygen and carbon), and possible evaporated filament material (W, Ta) immediately after preparation, by scanning the region from 0 to 1280 eV binding energy. In addition to the wide scans, 20-eV scans of the O 1s and C 1s regions were monitored. The only contamination observed in these experiments was oxygen. The spectra reported here are from specimens on which no oxygen signal could be observed initially. Some of the metals showed oxygen buildup in the course of the measurements; however, no photoemission lines were detected from the formation of an oxide, even from samples with the largest oxygen 1s signals. Whenever the

oxygen signal reached a level of  $\sim 0.5$  monolayer coverage, a new sample was prepared.<sup>30,31</sup> The average time for the measurement of a valence band spectrum was about 8 h, while scandium specimens could be kept in the spectrometer vacuum for over 24 h with no detectable oxygen buildup; the chromium samples had to be recleaned after about 1 h of running. The number of counts per channel on the valence band spectra reflects the length of time the sample could be studied. For the chromium runs, the Cr  $2P_{3/2}$  and the O 1s lines were scanned before and after each run. This enabled us to use the relative photoionization cross sections reported by Leckey<sup>32</sup> to ascertain the oxygen contamination. The ratios of the peak heights of the Cr  $2P_{3/2}$  to the O 1s peak was greater than 20 after each of the runs that are incorporated in the final spectrum. These individual runs, although suffering from poor statistics, seemed to give undistorted valence-band spectra and when added gave a spectrum identical to the one reported here.

## III. RESULTS

The XPS spectra  $I(E)$  of the valence-band regions of the transition metals reported here, Sc through Fe, are shown in Figs. 1 and 2. In these spectra each point represents the sum of the counts in four adjacent channels. The solid curves are straight-line segments, joining the experimental points. Structural features (i.e., characteristic peaks, shoulders, and edges) of the XPS valence band spectra  $I(E)$  of each element are denoted by letters in Figs. 1 and 2 and the energies (referred to the Fermi level  $E_F$ ) are given in Table I. Sharp decreases in intensity at the Fermi level in Sc, Co, Ni, and Au define  $E_F$  to better than  $\pm 0.05$  eV in a single determination. However, instrumental drift over the course of these runs necessitated repeated determination of the Fermi level. We used the above standards, cross checked the reported Fermi levels of the samples, and used our known instrumental resolution as a check of

TABLE I. Energies of characteristic features in the valence band spectra of the transition metals. Errors are given parenthetically. Entries are in eV.

Element	A	B	C	D	E
Sc	0.4(1)	1.4(2)	3.6(3)	5.6(3)	8.3(4)
Ti	0.7(1)	1.7(2)	4.2(2)	...	8.1(3)
V	0.6(1)	2.4(2)	5.0(3)	...	9.1(3)
Cr	1.8(1)	2.6(2)	3.5(3)	...	8.8(3)
Mn	1.1(1)	4.1(3)	...	...	8.7(4)
Fe	0.8(1)	1.9(2)	4.9(5)	...	9.2(4)

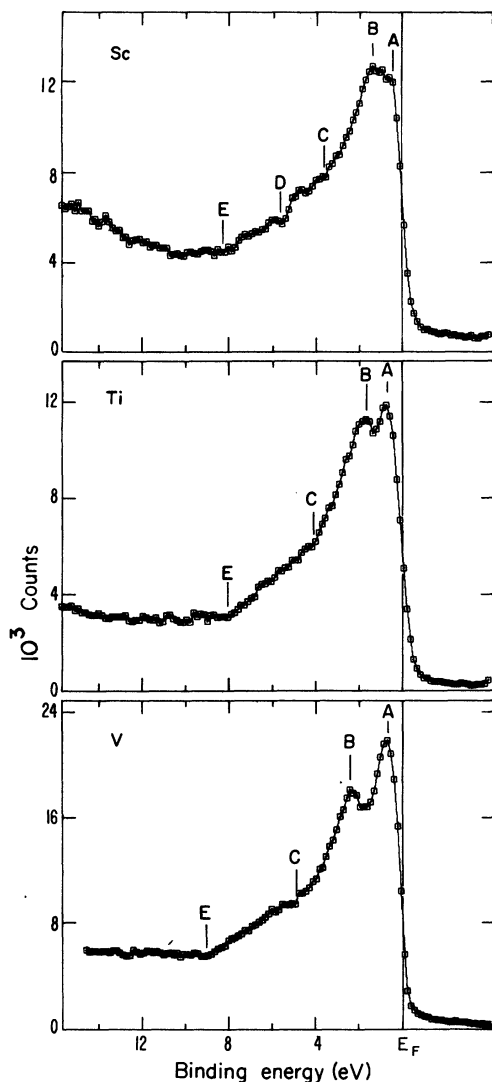


FIG. 1. X-ray-photoemission spectrum  $I(E)$  of the valence-band region of Sc, Ti, and V. The sum of the counts in four adjacent channels is represented by points joined with straight lines. The points are approximately 0.16 eV apart. The features, denoted by letters, are discussed in the text and the energies are given in Table I.

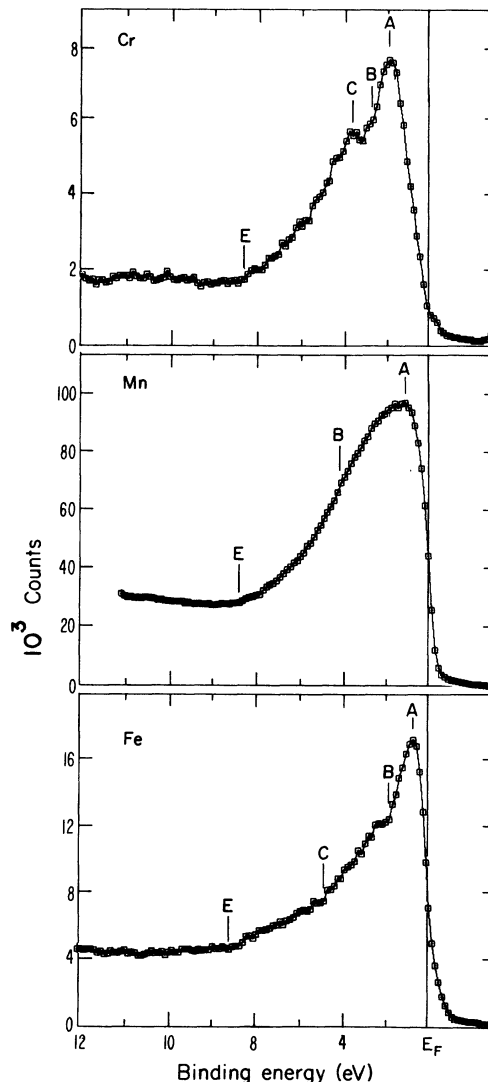


FIG. 2. X-ray-photoemission spectrum  $I(E)$  of the valence band region of Cr, Mn, and Fe. The sum of the counts in four adjacent channels is represented by points joined with straight lines. The points are approximately 0.16 eV apart. The features, denoted by letters, are discussed in the text and the energies are given in Table I.

our determination of the Fermi levels. The uncertainty in the reported Fermi level is  $\sim \pm 0.05$  eV for all samples except Cr, where the uncertainty in the value of the Fermi level is  $\sim \pm 0.10$  eV.

At the other end of the valence-bands—the “bottom” or high binding energy limit—it is more difficult to establish exactly where the bands end, although XPS spectra tend to be more readily interpretable in this respect than either SXS or UPS data. Most of our spectra show some tailing at the “bottom” of the valence bands. This tailing

may be a real physical effect for it persists even after subtraction of the inelastic tail through the assumption that each point in  $I(E)$  contributes to the inelastic tail in proportion to its initial intensity. In any case, some interpretation is necessary to assign the positions of the bottoms of the valence bands. The bottom of the valence bands for Sc and Fe is well defined by the negative curvature in  $I(E)$  in this region. The spectra of Ti through Mn exhibit a slight kink as  $I(E)$  joins the essentially flat background.

## IV. DISCUSSION

## A. Comparison with other experimental results

In this section we present a short comparison of our XPS spectra with other XPS measurements and with lower photon energy ( $h\nu \leq 40$  eV) experiments—namely UPS and SXS.

In Fig. 3 we compare the VB spectra of Cr obtained through the use of the UPS, SXS, and XPS methods. The SXS was obtained by Fischer<sup>4</sup>; it represents the Cr ( $2p$  hole)–Cr (VB hole) transitions. The UPS spectrum is from Eastman<sup>13</sup> at photon energy of 10.2 eV and the XPS spectrum is from this work. The three spectra indicate a region of high electron intensity around  $-2.0$  eV and similar band full width at half maximum (FWHM) of 4.9 eV (XPS), 4.6 eV (UPS), and 4.5 eV (SXS). The energies of the fine structure in these spectra vary considerably from one method to the other. Also, more recent UPS spectra of<sup>33</sup> Cr taken with the He I and He II lines have different appearances from those in Fig. 3. For Ti, the SXS spectrum taken by Fischer and Baun<sup>7</sup> does not agree well with XPS and UPS data, which agree with each other quite well in this case. Similarly for Fe,<sup>13,21,34</sup> Pessa *et al.*<sup>21</sup> had good agreement between their UPS spectrum at 16.84 eV and the XPS spectrum.

It can be concluded, therefore, that the degrees of actual correspondence of UPS and XPS spectra

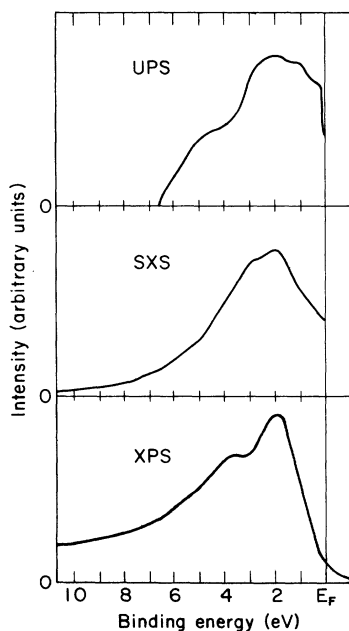


FIG. 3. Comparison of the valence-band spectra of Cr obtained by UPS (Ref. 13), SXS (Ref. 4) and XPS (this work).

can be interpreted as a measure of the structure introduced into the UPS spectrum by the final states along with the differences in cross-section modulation in the two energy regimes.

Our present XPS results agree quite well with earlier XPS data on Fe, in particular those of Refs. 26 and 27. The spectrum reported by Szalowski and Megerle<sup>25</sup> is not in as good an agreement. Our Mn spectrum has slightly better statistics than that reported by Hüfner and Wertheim<sup>27</sup>; however, the agreement between the two spectra is quite good.

## B. Comparison with theory

In comparing our spectra with the theoretical density of states  $N(E)$  obtained through band structure calculations, we will assume that the "density of ionization potentials," our measured  $I(E)$ , resembles  $N(E)$ . The implications of this assumption have been discussed elsewhere<sup>15,23,35</sup> and will not be reported here. At the same time, we note that attempts to interpret  $I(E)$  in terms of  $N(E)$  may be regarded as a test of the applicability of this procedure.

In the following we will compare our XPS spectra separately with theoretical results for each of the metals studied.

## 1. Scandium and titanium

Scandium and titanium start the  $3d$  transition-metal series with atomic configurations  $3d^1 4s^2$  and  $3d^2 4s^2$ , respectively. They both crystallize in an hcp lattice with a  $c/a$  ratio of 1.59.

This structural identity introduces an element of rigidity into the band structure, which is borne out quite clearly in the high-energy part of  $I(E)$ , if we line up the shoulders of the peaks labeled  $B$  in  $I(E)$  for scandium and titanium (compare Fig. 1). Between peak  $B$  and the Fermi level  $E_F$ ,  $I(E)$  rises to form a second peak in Ti while scandium  $E_F$  intersects  $N(E)$  before the peak is reached. Finite resolution of the spectrometer moves the break in intensity to a point 0.4 eV below  $E_F$ . The titanium valence bands have to accommodate one more electron, and  $E_F$  is accordingly shifted up 0.5 eV. Thus, the second peak  $A$  in the density of states is occupied beyond its maximum and  $E_F$  intersects a region of lower density, with the break in  $I(E)$  again shifted down 0.4 eV by instrumental broadening.

Toward lower energy,  $I(E)$  tails off in a similar way for both metals. The bottom of the valence bands is, in each case, tentatively assigned to a kink  $E$  which occurs at approximately  $E_F - 8.3$  eV for Sc and  $E_F - 8.1$  eV for Ti.

A closer inspection reveals some important differences in detail. Between peak  $B$  and edge  $D$ ,

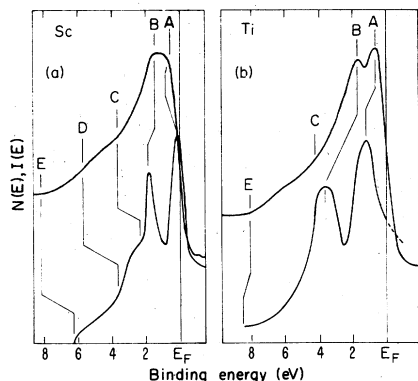


FIG. 4. Comparison of the x-ray-photoemission valence band spectra  $I(E)$  (upper curves) with density of states  $N(E)$  (lower curves) calculated by Altmann and Bradley (Refs. 36 and 37) for Sc and Ti. The energies of the characteristic features are given in Table II.

the scandium spectrum tails off in an  $s$ -like shape with an inflection point  $C$  around  $\sim 4$  eV. In titanium, we can just distinguish a discontinuity in slope marked  $C$  in Fig. 1.

The density of states  $N(E)$  for scandium and titanium has been calculated by Altmann and Bradley<sup>36,37</sup> using the cellular method. We compare their results with our spectra in Fig. 4. The energies of characteristic features are set out in Table II.

The agreement in the overall shape of  $N(E)$  and  $I(E)$  is good for Sc and fair for Ti. Notice especially the two peaks  $A$  and  $B$  and the change in position of  $E_F$  relative to peak  $A$  from scandium to titanium. The repeated changes in the curvature of  $I(E)$  between  $B$  and  $E$  in scandium as opposed to the essentially smooth decrease of  $I(E)$  in the same region in titanium agree quite well with the Altmann and Bradley calculation. The lack of resolution in their  $N(E)$  histograms, however, obviates the identification of feature  $C$  in the titanium spectrum.

This quite satisfactory overall picture is marred by considerable discrepancies in the energies of characteristic features between  $N(E)$  and  $I(E)$ , the exception being the total bandwidth of titanium (compare Table II). The different directions in which the upper and lower parts of  $N(E)$  deviate from their experimental counterparts may reflect the different origins of the regions in terms of atomic orbitals. These differences make the matching of features  $C$  and  $D$  in  $I(E)$  for scandium with similar ones in  $N(E)$  rather arbitrary.

Mattheiss<sup>38</sup> has calculated the band structure of titanium along the  $\Gamma$ - $K$  symmetry direction using the augmented-plane-wave (APW) method. His total bandwidth of 6.3 eV falls considerably short

TABLE II. Comparison of structural features in the valence band spectrum of scandium and titanium with the corresponding densities of states calculated by Altmann and Bradley (Refs. 34,35). The entries are in eV below the Fermi energy  $E_F$ . Errors are given parenthetically.

	Sc		Ti	
	Experiment	Theory	Experiment	Theory
$E_F$	0	0	0	0
Peak A	0.4(1)	0.0	0.7(1)	1.0
Peak B	1.4(2)	1.7	1.7(2)	3.4
Inflection point C	3.6(3)	2.4	4.2(2)	...
Inflection point D	5.6(3)	3.6 <sup>a</sup>	...	...
Bottom of VB E	8.3(4)	6.0	8.1(3)	8.0

<sup>a</sup>The identification of features  $C$  and  $D$  in  $N(E)$  is ambiguous (see text).

of the 8.1 eV measured in this experiment. Hygh and Welch<sup>39</sup> have also done several APW calculations on Ti. Their bandwidths also fall short of experiment, but their density of states does show a two-peak structure. It would be interesting to compare our results with more recent APW<sup>40</sup> and linear-combination-atomic-orbitals<sup>41</sup> (LCAO) calculations when the calculated densities become available. The APW bands calculated for Sc by Fleming and Loucks<sup>42</sup> are likewise considerably narrower than observed. Das *et al.*<sup>43</sup> have recently performed a relativistic APW calculation on Sc. Their density of states compares qualitatively with our XPS results but again are much too narrow.

## 2. Vanadium and chromium

Vanadium and chromium, with 5 and 6 valence electrons, respectively, crystallize in the relatively open body-centered cubic (bcc) structure.

Chromium is an antiferromagnet at room temperature with a spin arrangement in the form of a spin-density wave. The wavelength is slightly less than twice the periodicity of the chemical lattice. Disregarding this difference, Asano and Yamashita<sup>44</sup> have treated the band structure of an idealized antiferromagnetic chromium by invoking the concept of a magnetic superlattice with twice the ordinary lattice constant. This reduces the Brillouin zone (BZ) of the bcc lattice and introduces gaps of the order of 0.4 eV at points where bands cross the new zone boundaries. Though the occurrence of these gaps at the Fermi energy is es-

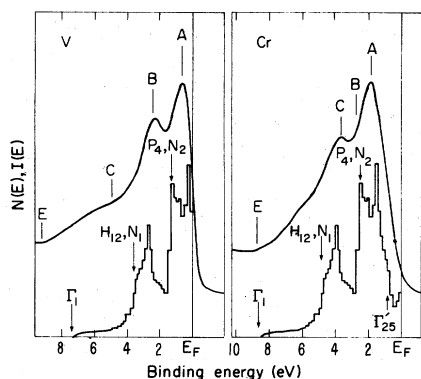


FIG. 5. X-ray-photoemission valence-band spectra  $I(E)$  of V and Cr are compared with the APW results of Gupta and Sinha (Ref. 47). For V we have used Gupta and Sinha's Cr density of states with the Fermi level shifted corresponding to the reduction of the number of valence electrons by one electron.

essential for the stabilization of the antiferromagnetic order<sup>45</sup> in Cr, we do not expect them to alter the overall density of states strongly because they occur at different energies for different bands. This explains the great similarity in the densities of states derived by Connolly<sup>46</sup> for the band-structure calculations of paramagnetic and antiferromagnetic Cr by Asano and Yamashita.<sup>44</sup> It is therefore reasonable to compare our measurements with calculations on the paramagnetic state of bcc chromium.

Densities of states  $N(E)$  have been calculated by several authors. The best agreement between theory and experiment is found in the APW calculations by Gupta and Sinha,<sup>47</sup> shown in Fig. 5. The overall agreement between  $N(E)$  and our experimental spectrum is quite good. The edge at 4.9 eV in  $N(E)$  marks the position of the symmetry points  $H_{12}$  and  $N_1$  and thus the bottom of the  $d$  bands. The spike in  $N(E)$  at 2.4 eV arises from

the flat bands connecting  $P_4$  and  $N_2$  along the  $PN$  edge of the bcc Brillouin zone. The high spike at 1.4 eV on  $N(E)$  is not readily attributable to any particular region in the BZ. In agreement with the band-structure calculation, we find that  $I(E)$  is quite low near  $E_F$ . This feature has not been previously observed by the UPS or SXS methods.

A tail due mainly to a  $4s$ -derived band extends down to 8.5 eV in  $N(E)$ . This agrees reasonably well with the value  $8.8 \pm 0.3$  eV determined for the total valence bandwidth of chromium from our spectrum. The  $d$ -band densities of states calculated by Asdente and Friedel<sup>48</sup> using a tight-binding scheme agrees in general shape with our spectrum, as does the APW calculation of Snow and Waber.<sup>49</sup> Energies of symmetry points from four recent calculations<sup>47,50,51</sup> are compared with values deduced from our spectrum in Table III. It is clear from this that the agreement between the different theories and our spectrum is rather good, though the tight-binding calculations<sup>50,51</sup> give narrower bands.

The valence-band spectrum of vanadium is very similar to that of chromium. Allowing for a shift in the Fermi level  $E_F$  due to the reduction by one in the number of valence electrons, we find a one-to-one correspondence in the characteristic features of the two spectra. In vanadium,  $E_F$  has moved down toward the higher peak by about 1 eV. The separation between the two main peaks is almost the same of about 1.8 eV. In vanadium, both peaks appear narrower. This reduction in  $d$ -band dispersion is presumably due to the slightly increased atomic spacing of vanadium as compared to chromium. In Fig. 5 we compare the Cr density of states of Gupta and Sinha,<sup>47</sup> shifted toward  $E_F$  by 1 eV, with our vanadium spectrum. Peak A marks the maximum near symmetry points  $P_4$  and  $N_2$ . The energies of  $H_{12}$  and  $N_1$  at the bottom of the  $d$  bands are well defined in the vanadium spectrum at  $3.5 \pm 0.3$  eV below  $E_F$ . The detailed picture that

TABLE III. Energies of symmetry points in the valence bands of chromium (eV below  $E_F$ ).

Symmetry point	Tight-binding plus OPW <sup>a</sup>		Tight-binding, SCF <sup>b</sup>	APW, $\alpha = 1$ <sup>c</sup>	Experiment, this work
	$\alpha = 1$	$\alpha = 0.725$	$\alpha = \frac{2}{3}$		
$\Gamma'_{25}$	1.0	1.0	1.0	0.7	
$P_4$	1.6	2.0	2.2	2.5	2.6(2)
$N_2$	2.3	2.4	2.7	2.4	
$H_{12}$	3.0	3.3	4.0	4.8	3.5(3)
$N_1$	3.3	3.9	4.3	4.9	
$\Gamma_1$	5.1	6.9	5.9	8.7	8.8(3)

<sup>a</sup>Orthogonalized plane wave (Ref. 50). Here  $\alpha$  is the exchange parameter.

<sup>b</sup>Self-consistent field (Ref. 51).

<sup>c</sup>Reference 47.

we have obtained for the density of the states of Cr and V will aid us in interpretation of the Fe spectrum.

### 3. Manganese

Manganese crystallizes in a distorted cubic lattice with 29 atoms per primitive cell. No band structure has therefore as yet been calculated. The VB spectrum (see Fig. 2) shows a broad bump with a total width of  $8.8 \pm 0.3$  eV. A peak *A* at  $E_F - 1.1$  eV and a shoulder *B* at  $E_F - 4.1$  eV can be distinguished in  $I(E)$ . Judging from the steep slope at  $E_F$ , the density at  $E_F$  is probably close to its maximum value.

### 4. Iron

The band model of ferromagnetism due to Stoner, Wohlfarth, and Slater<sup>52,53</sup> (SWS) features spin-polarized bands  $\epsilon_n(\mathbf{k})$  which are split by energies  $\Delta E_n(\mathbf{k})$  due to the exchange interaction.  $\Delta E$  is a function of wave vector  $\mathbf{k}$  and band index  $n$  but it has usually been treated as a constant for *d*-derived bands and is set equal to zero for *sp*-derived bands. Estimates<sup>54</sup> for the average exchange splitting of the *d* bands  $\Delta E$  are about 0.4 eV in Ni, 1.1 eV in Co, and 1.7 eV in Fe.

More recently, band-structure calculations of ferromagnetic Fe by Tawil and Callaway<sup>55</sup> have derived the exchange splitting  $E_n(\mathbf{k})$  self-consistently, using an average Hartree-Fock field that is different for the two electron spin directions. These calculations reproduce the observed saturation moments quite satisfactorily.

Schemes different from the SWS model have been proposed<sup>56</sup> which emphasize intra-atomic exchange

and correlation effects in the formation of spin-ordered structures. However, to our knowledge, no explicit calculations have been made which would bear directly on the electronic structure of ferromagnetic transition metals.

Two of the implications of the SWS model have been tested extensively: (i) The spin polarization of electrons at the Fermi energy  $E_F$  is well established<sup>57,58</sup> and can be explained both in sign and magnitude by the SWS model.<sup>59</sup> (ii) A number of spectroscopic techniques have been employed to study the changes in the band structure which are supposed to accompany the transition from the ferromagnetic to the paramagnetic state as  $\Delta E$  goes to zero at the Curie temperature  $T_C$ .<sup>5,8,34,60,61</sup> The effects observed are, however, very small and do not readily lend themselves to a straightforward interpretation in terms of the SWS model.

In this situation let us rephrase the question put forward by previous investigators from: "Does the band structure of a metal change according to the SWS model if we cross the Curie temperature  $T_C$ ?" to "Does the SWS model give an appropriate description of the density of states  $N(E)$  of a ferromagnetic transition metal, like iron, below  $T_C$ ?"

It is interesting to note that since iron and chromium crystallize in the same bcc structure and have only slightly different lattice constants, we may regard the  $N(E)$  curve for chromium (Fig. 5) as a fair representation of  $N(E)$  for iron in the unmagnetized state. The Fermi energy  $E_F$  for this state would fall right at the top of the high-density peak, as shown in Fig. 6(a). The chemical potentials for spin up ( $\lambda_+$ ) and spin down ( $\lambda_-$ ) can easily be determined by allowing for the appropriate magnetic moment in ferromagnetic iron and assuming a rigid-band exchange splitting  $\Delta E$ . In the final step,  $\lambda_+$  and  $\lambda_-$  coincide to form the new Fermi level in the SWS description of the ferromagnetic state. It is clear from Fig. 6(b) that this new density of states differs drastically from the nonpolarized  $N(E)$ . Instead of a peak, we now have a region of low electron density at  $E_F$  and a peak about 1.8 eV below  $E_F$ .

These two features are common to all  $N(E)$  calculations for Fe employing the SWS model and we find just these features in our XPS spectrum of iron, shown in Fig. 7 together with  $N(E)$  derived by Connolly<sup>46</sup> from the energy bands of Wakoh and Yamashita.<sup>62</sup>

As can be seen from Fig. 7, the agreement is quite good and details are well reproduced. The bottom of the *d* bands is marked, in Connolly's and in Tawil and Callaway's calculations, by an edge in  $N(E)$  between 4.5 and 5.0 eV. Structure *C* in  $I(E)$ , which presumably corresponds to this point, lies at least 0.5 eV lower. The bottom of

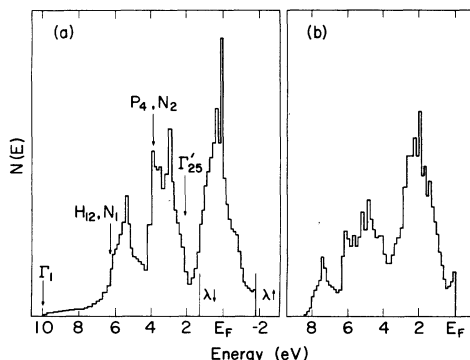


FIG. 6. (a) bcc chromium density of states (Ref. 47)  $\lambda_+$  and  $\lambda_-$ , the spin up and spin down chemical potentials for bcc Fe are determined from the magnetic moment of Fe under the assumption of a rigid band exchange splitting. (b) The resulting spin-polarized density of states where the chemical potentials  $\lambda_+$  and  $\lambda_-$  have been made to coincide. This density of states should be representative for that of ferromagnetic iron.

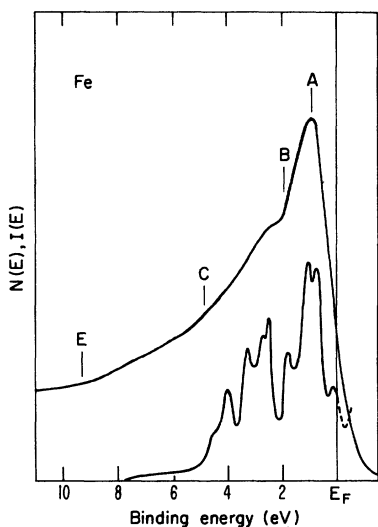


FIG. 7. Comparison of the x-ray-photoemission valence-band spectrum  $I(E)$  of Fe (upper curve) with the  $N(E)$  derived by Connolly (Ref. 46) (lower curve).

the valence bands is marked at 9.2 eV by the intercept of the parabolic  $sp$  band with the baseline. The calculated values for the same point  $\Gamma_1$  again fall short of this value by about 1.4 eV.

A very detailed treatment of the exchange prob-

lem in the band structure of ferromagnetic iron has been given by Duff and Das.<sup>68</sup> As a result they obtained significantly greater exchange splittings throughout the Brillouin zone as compared to other calculations. This increased the overall bandwidth to 13 eV and the  $d$  bandwidth [point C in  $I(E)$ ] to 9.9 eV, both of which exceed the experimental values considerably. It is, however, clear from their calculation how assumptions about screening and the localizing effect of correlation influence the exchange and therefore the bandwidths. With the data provided by our spectrum we hope that information about the real magnitude of these many-body effects for the ferromagnetic state may be obtained.

Returning to the question of whether the SWS model is appropriate for describing  $N(E)$  for ferromagnetic metals below  $T_C$ , we note that, comparing Fig. 6 with Connolly's spectrum, the general features of Connolly's spectrum were reproduced to within an energy scale factor. This, plus similar agreements for our XPS spectra for Ni and Co,<sup>24</sup> lead us to believe that the answer is "yes."

#### ACKNOWLEDGMENTS

We would like to thank Professor Gabor Somorjai for the gift of the Cr and V single crystals and Dr. H. Nadler for the gift of the Ti single crystal.

<sup>†</sup>Work done with support from the U.S. ERDA.

\*Permanent address: Max-Planck Institut für Festkörperforschung, Stuttgart, West Germany.

<sup>‡</sup>On leave (1976-77) from University of Petroleum and Minerals, Dhahran, Saudi Arabia.

<sup>§</sup>Permanent address: Dept. of Chemistry, Massachusetts Institute of Technology, Cambridge, Mass.

<sup>1</sup>L. Hodges, R. E. Watson, and H. Ehrenreich, *Phys. Rev. B* **5**, 3953 (1972).

<sup>2</sup>For a review see C. Herring, in *Magnetism*, edited by G. T. Rado and H. Suhl (Academic, New York, 1966), Vol. IV.

<sup>3</sup>D. W. Fischer, *J. Appl. Phys.* **40**, 4151 (1969).

<sup>4</sup>D. W. Fischer, *Phys. Rev. B* **4**, 1778 (1971).

<sup>5</sup>R. C. Dobbyn, M. L. Williams, J. R. Cuthill, and A. J. McAlister, *Phys. Rev. B* **2**, 1563 (1970).

<sup>6</sup>A. J. McAlister, J. R. Cuthill, R. C. Dobbyn, M. L. Williams, and R. E. Watson, *Phys. Rev. Lett.* **29**, 179 (1972); *Phys. Rev. B* **12**, 2973 (1975).

<sup>7</sup>D. W. Fischer and W. L. Baun, *J. Appl. Phys.* **39**, 4757 (1968).

<sup>8</sup>D. T. Pierce and W. E. Spicer, *Phys. Rev. Lett.* **25**, 581 (1970).

<sup>9</sup>C. N. Berglund and W. E. Spicer, *Phys. Rev.* **136**, A1030 (1964); **136**, A1044 (1964).

<sup>10</sup>A. J. Blodgett, Jr., and W. E. Spicer, *Phys. Rev.* **146**, 390 (1966).

<sup>11</sup>A. Y.-C. Yu and W. E. Spicer, *Phys. Rev. Lett.* **23**, 1171 (1966).

<sup>12</sup>A. J. Blodgett and W. E. Spicer, *Phys. Rev.* **153**, 514 (1967).

<sup>13</sup>D. E. Eastman, *J. Appl. Phys.* **40**, 1387 (1969).

<sup>14</sup>D. E. Eastman, *Solid State Commun.* **7**, 1697 (1969);

D. E. Eastman, in *Electron Spectroscopy*, edited by D. A. Shirley (North-Holland, Amsterdam, 1972), p. 487.

<sup>15</sup>C. S. Fadley and D. A. Shirley, *Spec. Publ. Natl. Bur. Stand. (U.S.)* **323**, 163 (1971).

<sup>16</sup>G. D. Mahan, *Phys. Rev.* **163**, 612 (1967); C. Kunz, R. Haensel, G. Keitel, P. Schreiber, and B. Sonntag, *Spec. Publ. Natl. Bur. Stand. (U.S.)* **323**, 253 (1971).

<sup>17</sup>See, for example, W. E. Spicer, *Spec. Publ. Natl. Bur. Stand. (U.S.)* **323**, 139, 191 (1971); and P. J. Feibelman and D. E. Eastman, *Phys. Rev. B* **12**, 4932 (1974).

<sup>18</sup>See, for example, W. F. Krolkowski and W. E. Spicer, *Phys. Rev.* **185**, 882 (1969).

<sup>19</sup>(a) N. V. Smith, *Spec. Publ. Natl. Bur. Stand.* **323**, 191 (1971). (b) M. M. Traum and N. V. Smith, *Phys. Rev. B* **9**, 1353 (1974).

<sup>20</sup>A. R. Williams, J. F. Janak, and V. Moruzzi, *Phys. Rev. Lett.* **28**, 671 (1972).

<sup>21</sup>M. Pessa, P. Heimann, and H. Neddermeyer, *Phys. Rev. B* **14**, 3488 (1976).

<sup>22</sup>D. E. Eastman and W. D. Grobman, *Phys. Rev. Lett.* **28**, 1327 (1972).

<sup>23</sup>L. Ley, R. A. Pollak, F. R. McFeely, S. P. Kowalczyk, and D. A. Shirley, *Phys. Rev. B* **9**, 600 (1974).

<sup>24</sup>L. Ley, S. P. Kowalczyk, F. R. McFeely, and D. A.



- Shirley, Lawrence Berkeley Laboratory Report No. 2929, 1974 (unpublished).
- <sup>25</sup>F. J. Szalkowski and C. A. Megerle, Phys. Lett. A 48, 117 (1974).
- <sup>26</sup>H. Höchst, A. Goldman, and S. Hüfner, Z. Phys. B 24, 245 (1976).
- <sup>27</sup>S. Hüfner and G. K. Wertheim, Phys. Lett. A 47, 349 (1974).
- <sup>28</sup>Y. Baer, P. F. Hedén, J. Hedman, M. Klasson, C. Nordling, and K. Siegbahn, Phys. Scr. 1, 55 (1970).
- <sup>29</sup>R. A. Pollak, S. P. Kowalczyk, L. Ley, and D. A. Shirley, Phys. Rev. Lett. 29, 274 (1972).
- <sup>30</sup>T. E. Madey, J. T. Yates, and N. E. Erickson, Chem. Phys. Lett. 19, 487 (1973).
- <sup>31</sup>D. R. Penn, J. Electron Spectrosc. Relat. Phenom. 19, 29 (1976).
- <sup>32</sup>R. C. G. Leckey, Phys. Rev. A 13, 1043 (1976).
- <sup>33</sup>P. J. Page and P. M. Williams, in *Vacuum Ultraviolet Radiation Physics*, edited by E. Koch, R. Haensel, and C. Kunz (Pergamon-Vieweg, New York, 1974), p. 566.
- <sup>34</sup>L.-G. Petersson, R. Melander, D. P. Spears, and S. B. M. Hagström, Phys. Rev. B 14, 4177 (1976).
- <sup>35</sup>L. Ley, S. P. Kowalczyk, F. R. McFeely, R. A. Pollak, and D. A. Shirley, Phys. Rev. B 8, 2392 (1973).
- <sup>36</sup>S. L. Altmann and C. J. Bradley, Proc. Phys. Soc. Lond. 92, 764 (1967).
- <sup>37</sup>S. L. Altmann and C. J. Bradley, in *Soft X-Ray Band Spectra*, edited by D. J. Fabian (Academic, New York, 1968), p. 265.
- <sup>38</sup>L. F. Mattheiss, Phys. Rev. 134, A970 (1964).
- <sup>39</sup>E. H. Hygh and R. M. Welch, Phys. Rev. B 1, 2424 (1970); R. M. Welch and E. H. Hygh, *ibid.* 4, 4261 (1971); 9, 1993 (1974).
- <sup>40</sup>R. A. Tawil and J. Rath (private communication).
- <sup>41</sup>R. A. Tawil and T. J. Green, Arab. J. Sci. Engin. 2, 113 (1977).
- <sup>42</sup>G. S. Fleming and T. L. Loucks, Phys. Rev. 173, 685 (1968).
- <sup>43</sup>S. G. Das, A. J. Freeman, D. D. Koelling, and F. M. Mueller, AIP Conf. Proc. 18, 1304 (1973).
- <sup>44</sup>S. Asano and J. Yamashita, J. Phys. Soc. Jpn. 23, 714 (1967).
- <sup>45</sup>W. M. Lomer, in *Proceedings of the International School of Physics, Enrico Fermi, Course XXXVII*, edited by W. Marshall (Academic, New York, 1967).
- <sup>46</sup>J. W. D. Connolly, *Electronic Density of States*, Spec. Publ. Natl. Bur. Stand. (U.S. GPO, Washington, D. C., 1971), Vol. 323, p. 27.
- <sup>47</sup>R. P. Gupta and S. K. Sinha, Phys. Rev. B 3, 2401 (1971).
- <sup>48</sup>M. Asdente and J. Friedel, Phys. Rev. 124, 384 (1961).
- <sup>49</sup>E. C. Snow and J. T. Waber, Acta Metall. 17, 623 (1969).
- <sup>50</sup>M. Yasin, E. Hayashi, and M. Shimiga, J. Phys. Soc. Jpn. 29, 1440 (1970).
- <sup>51</sup>J. Rath and J. Callaway, Phys. Rev. B 8, 5398 (1973).
- <sup>52</sup>E. C. Stoner, Philos. Mag. 15, 1018 (1933); E. P. Wohlfarth, Rev. Mod. Phys. 25, 211 (1953).
- <sup>53</sup>J. C. Slater, Phys. Rev. 49, 537, 931 (1936).
- <sup>54</sup>E. P. Wohlfarth, *Proceedings of the International Conference on Magnetism* (Institute of Physics and Physical Society of London, Nottingham, England, 1965), p. 51.
- <sup>55</sup>R. A. Tawil and J. Callaway, Phys. Rev. B 7, 1242 (1973); C. S. Wang and J. Callaway (unpublished).
- <sup>56</sup>See, for example, J. H. Van Vleck, Rev. Mod. Phys. 25, 220 (1953).
- <sup>57</sup>W. Eib and S. F. Alvarado, Phys. Rev. Lett. 37, 444 (1976).
- <sup>58</sup>M. Landolt and M. Campagne, Phys. Rev. Lett. 38, 663 (1977).
- <sup>59</sup>B. A. Politzer and P. H. Cutler, Phys. Rev. Lett. 28, 1330 (1972); J.-N. Chazalviel and Y. Yafet, Phys. Rev. B 15, 1062 (1977).
- <sup>60</sup>C. S. Fadley and D. A. Shirley, Phys. Rev. Lett. 21, 980 (1968).
- <sup>61</sup>J. E. Rowe and J. C. Tracy, Phys. Rev. Lett. 27, 799 (1971).
- <sup>62</sup>S. Wakoh and J. Yamashita, J. Phys. Soc. Jpn. 21, 1712 (1966).
- <sup>63</sup>K. J. Duff and T. P. Das, Phys. Rev. B 3, 192 (1971).